



Numerical modelling of modular high-temperature gas-cooled reactors with thorium fuel

Mikołaj Oettingen ,
Jerzy Cetnar

Abstract. The volumetric homogenization method for the simplified modelling of modular high-temperature gas-cooled reactor core with thorium-uranium fuel is presented in the paper. The method significantly reduces the complexity of the 3D numerical model. Hence, the computation time associated with the time-consuming Monte Carlo modelling of neutron transport is considerably reduced. Example results comprise the time evolutions of the effective neutron multiplication factor and fissionable isotopes (^{233}U , ^{235}U , ^{239}Pu , ^{241}Pu) for a few configurations of the initial reactor core.

Keywords: HTR • Homogenization • Thorium • Monte Carlo

Introduction

The design of the nuclear reactor core requires the application of complex methods for reliable reconstruction of the geometry and material composition of the actual reactor core. The greater the complexity of the core geometry is, the longer the computation time of neutron transport will be, especially when using Monte Carlo methods. Additionally, the execution of many input files with varied key parameters is necessary for a comprehensive parametric study. The problem is particularly significant in the modelling of modular high-temperature gas-cooled reactors (MHTRs) with graphite fuel compacts containing spherical TRi-structural ISOtropic (TRISO) particles, called double heterogeneity [1]. In the paper, an alternative method called volumetric homogenization is presented for reducing complexity of the numerical model and the resulting computation time. The method assumes the elimination of double heterogeneity of TRISO particles embedded in the fuel compact. In this method, materials of TRISO particles are admixed to the graphite matrix of the compact and by this way, the complicated geometrical structure of multilayer TRISO particles is eliminated and replaced by one homogenized

M. Oettingen
AGH University of Science and Technology
Faculty of Energy and Fuels
Mickiewicza 30 Ave., 30-059 Krakow, Poland
E-mail: moettin@agh.edu.pl

J. Cetnar
National Centre for Nuclear Research
Andrzeja Sołtana 7 Str., 05-400 Otwock-Świerk, Poland

Received: 17 December 2020

Accepted: 8 January 2021

0029-5922 © 2021 The Author(s). Published by the Institute of Nuclear Chemistry and Technology.
This is an open access article under the CC BY-NC-ND 4.0 licence (<http://creativecommons.org/licenses/by-nc-nd/4.0/>).

material. This, in turn, simplifies the numerical model and speeds up the simulations. The method was applied for the modelling of the MHTR core with thorium-uranium fuel [2, 3]. This kind of fuel mix is envisaged as an option for the currently designed nuclear reactors, including MHTR [4, 5]. Example results comprise the time evolutions of the effective neutron multiplication factor K_{eff} and of fissionable isotopes (^{233}U , ^{235}U , ^{239}Pu , ^{241}Pu) for a few configurations of the initial reactor core. The parametric study includes a variation of geometrical and material parameters of TRISO particles, i.e. kernel radius, packing fraction, enrichment etc. The numerical model of the reactor was developed using the Monte Carlo continuous energy burnup code (MCB) [6, 7]. In the next section, the volumetric homogenization method is comprehensively described. Section “Results” focuses on the design of numerical model and example results. The study is summarized in the last section.

Volumetric homogenization method

In this section, the volumetric homogenization method is described from the mathematical point of view. Table 1 shows the input parameters necessary to obtain the weight fractions of each isotope in the homogenized material mix and the density of the homogenized material for the Monte Carlo modelling of neutron transport. The presented mathematical set-up was transferred to the numerical script, which automatically calculates the aforementioned parameters using the input data from Table 1.

The calculations begin with the assessment of the volumes of each TRISO material in the fuel compact. The Appendix 1 contains list of symbols used in the applied equations. Initially, the volume of the spherical TRISO fuel kernel V^{KR} is calculated using Eq. (1), where r_{KR} is the kernel radius.

$$(1) \quad V^{\text{KR}} = \frac{4}{3} \pi \cdot r_{\text{KR}}^3$$

Next, the volumes V_i^{TRISO} of each TRISO material wrapping the kernel subsequently are calculated using Eq. (2). r_i is the kernel radius r_{KR} increased by the material layer thickness t_i , i.e. buffer porous carbon (BPC), inner pyrolytic carbon (IPyC), silicon

carbide (SiC) and outer pyrolytic carbon (OPyC), subsequently. For the calculating the volume of the BPC that is directly laid on the fuel kernel, it is known that r_{i-1} equals r_{KR} .

$$(2) \quad V_i^{\text{TRISO}} = \frac{4}{3} \pi \cdot (r_i^3 - r_{i-1}^3)$$

The volume V^{COM} of the cylindrical fuel compact is calculated using Eq. (3), where r_{COM} is the compact radius and h_{COM} is the compact height.

$$(3) \quad V^{\text{COM}} = \pi \cdot r_{\text{COM}}^2 \cdot h_{\text{COM}}$$

In addition, Eq. (1) is used for the calculation of the TRISO particle volume V^{TRISO} , where r_{KR} is replaced by the radius of the whole TRISO particle r_{TRISO} .

The volumes calculated above may be used in Eq. (4) for calculations of the number of TRISO particles in the fuel compact N^{TRISO} for a given packing fraction P . The packing fraction is defined as the overall volume of all TRISO particles in the compact in relation to the compact volume (Eq. (5)).

$$(4) \quad N^{\text{TRISO}} = P \cdot \frac{V^{\text{COM}}}{V^{\text{TRISO}}}$$

$$(5) \quad P = \frac{V^{\text{TRISOinCOM}}}{V^{\text{COM}}}$$

Then, the volume of all TRISO particles in the compact $V^{\text{TRISOinCOM}}$ and associated volume fractions of each material of TRISO in the compact $V_i^{\text{TRISO,FR}}$ may be calculated by using Eqs. (6) and (7):

$$(6) \quad V^{\text{TRISOinCOM}} = V^{\text{TRISO}} \cdot N^{\text{TRISO}}$$

$$(7) \quad V_i^{\text{TRISO,FR}} = \frac{V_i^{\text{TRISO}}}{V^{\text{COM}}}$$

Then, with the given densities of each material in the compact ρ_i^{COM} , it is possible to calculate the mass of each material in the compact m_i^{COM} and its weight fraction $w_i^{\text{COM,FR}}$ by means of Eqs. (8) and (9). m^{COM} is the total mass of the compact for a given number of TRISO particles; see Eq. (10).

$$(8) \quad m_i^{\text{COM}} = V_i^{\text{TRISO,FR}} \cdot \rho_i^{\text{COM}}$$

$$(9) \quad w_i^{\text{COM,FR}} = \frac{m_i^{\text{COM}}}{m^{\text{COM}}}$$

$$(10) \quad m^{\text{COM}} = \sum_{i=1}^n m_i^{\text{COM}}$$

For the input of the Monte Carlo simulations, the density of the homogenized compact ρ^{HOMO} is also needed. It can be calculated using given densities ρ_i^{COM} and the calculated density of the (U,Th)O₂ (Eq. (17)), using Eq. (11).

$$(11) \quad a_i^{\text{U}} = w_i^{\text{U}} \cdot \frac{\overline{M}^{\text{U}}}{M_i^{\text{U}}}$$

In the next step, the material isotopic composition in the fuel compact is calculated. Initially, the isotopic composition of (U,Th)O₂ dioxide for given weight fractions of each dioxide $w_i^{\text{(HM)O}_2\text{,FR}}$ in the dioxide mix is considered. The main input param-

Table 1. Input data for the volumetric homogenization method

A. Material data	
Uranium enrichment	
Natural abundances of isotopes	
Atomic weights of isotopes	
Weight fractions of each dioxide in the dioxide mix	
Densities of fuel and no-fuel materials	
B. Geometry	
TRISO kernel radius	
TRISO layers thickness	
TRISO packing fraction	
Fuel compact radius	
Fuel compact height	

eter is the isotopic composition of uranium with a defined enrichment in ^{235}U . The isotopic composition of uranium is usually given as a weight fraction of each uranium isotope w_i^{U} . The isotopic compositions of light TRISO materials and graphite matrix are defined by natural abundances, which correspond to atom fractions. Therefore, the isotopic composition of uranium should be recalculated to atom fractions, which was performed using Eq. (12). In the case of thorium, the following recalculation is not necessary since it mainly contains one isotope: ^{232}Th . a_i^{U} is the atom fraction of each uranium isotope, M_i^{U} is the atomic weight of each uranium isotope and \bar{M}^{U} is the average atomic weight for given enrichment, which is calculated using Eq. (13).

$$(12) \quad a_i^{\text{U}} = w_i^{\text{U}} \cdot \frac{\bar{M}^{\text{U}}}{M_i^{\text{U}}}$$

$$(13) \quad \bar{M}^{\text{U}} = \left(\sum_{i=1}^n \frac{w_i^{\text{U}}}{M_i^{\text{U}}} \right)$$

Further, the atom fractions $a_i^{(\text{HM})\text{O}_2}$ of each isotope in UO_2 and ThO_2 dioxides are calculated using Eq. (14), where the index HM corresponds to heavy metal (either U or Th). $N_i^{(\text{HM})\text{O}_2}$ is the average number of atoms of each isotope in the dioxide and $N^{(\text{HM})\text{O}_2}$ is the number of atoms in the dioxide molecule.

$$(14) \quad a_i^{(\text{HM})\text{O}_2} = \frac{N_i^{(\text{HM})\text{O}_2}}{N^{(\text{HM})\text{O}_2}}$$

Then, the atom fraction $a_i^{(\text{HM})\text{O}_2, \text{FR}}$ of each dioxide in the dioxide mix is calculated using Eq. (15). The weight fractions of each dioxide in the mix $w_i^{(\text{HM})\text{O}_2, \text{FR}}$ are given the input parameters. The atomic weights of each dioxide $M^{(\text{HM})\text{O}_2}$ are calculated using Eq. (16), while the average atomic weight of the mixed dioxides $\bar{M}^{(\text{HM})\text{O}_2, \text{MIX}}$ is calculated using Eq. (17), which is a modification of Eq. (13) for molecules.

$$(15) \quad a_i^{(\text{HM})\text{O}_2, \text{FR}} = w_i^{(\text{HM})\text{O}_2, \text{FR}} \frac{\bar{M}^{(\text{HM})\text{O}_2, \text{MIX}}}{M_i^{(\text{HM})\text{O}_2}}$$

$$(16) \quad \bar{M}^{(\text{HM})\text{O}_2} = M^{\text{HM}} + 2M^{\text{O}}$$

$$(17) \quad \bar{M}^{(\text{HM})\text{O}_2, \text{MIX}} = \left(\sum_{i=1}^n \frac{w_i^{(\text{HM})\text{O}_2, \text{FR}}}{M_i^{(\text{HM})\text{O}_2}} \right)$$

Afterwards, the density of mixed dioxides $\rho^{(\text{HM})\text{O}_2}$ for given densities of each dioxide $\rho_i^{(\text{HM})\text{O}_2}$ is calculated using Eq. (18) and it is further used for the calculation of the overall density of the homogenized material mix $\rho^{(\text{HM})}$ (Eq. (11)).

$$(18) \quad \rho^{(\text{HM})\text{O}_2} = \left(\sum_{i=1}^n \frac{w_i^{(\text{HM})\text{O}_2, \text{FR}}}{\rho_i^{(\text{HM})\text{O}_2}} \right)$$

Additionally, natural abundances of no-fuel compact and TRISO materials a_i^{ISO} should be recalculated in terms of weight fractions w_i^{ISO} , which was performed using Eq. (19).

$$(19) \quad w_i^{\text{ISO}} = a_i^{\text{ISO}} \frac{M_i}{M}$$

The last stage of calculations considers the preparation of the weight fractions of the homogenized material mix $w_i^{\text{HOMO,ISO}}$ and $w_i^{\text{HOMO, (HM)O}_2}$ for neutron transport Monte Carlo simulations. Further, $w_i^{\text{HOMO, (HM)O}_2}$ is calculated using Eq. (20), and $w_i^{\text{HOMO,ISO}}$ using Eq. (22).

$$(20) \quad w_i^{\text{HOMO, (HM)O}_2} = w_i^{\text{COM,FR}} \cdot w_i^{(\text{HM})\text{O}_2, \text{FR}} \cdot w_i^{(\text{HM})\text{O}_2}$$

$w_i^{(\text{HM})\text{O}_2}$ corresponds to the weight fractions of each isotope in the dioxide and it is calculated using Eq. (21). The $w_i^{\text{COM,FR}}$ fractions were calculated using Eq. (9).

$$(21) \quad w_i^{(\text{HM})\text{O}_2} = a_i^{(\text{HM})\text{O}_2} \cdot \frac{M^{(\text{HM})\text{O}_2}}{M_i^{(\text{HM})\text{O}_2}}$$

$$(22) \quad w_i^{\text{HOMO,ISO}} = w_i^{\text{COM,FR}} \cdot w_i^{\text{ISO}}$$

The weight fractions of carbon isotopes from different materials are finally summarized to simplify the input for numerical simulations and by this way, the final isotopic composition of the homogenized mix of fuel compact material was defined.

Results

The example calculations were performed for 180 MW_{th} MHTR core, as depicted in Fig. 1. The core comprises of 310 hexagonal fuel blocks including 60 blocks with control rods (CR) holes. The numerical Monte Carlo simulations were performed for a two-year irradiation cycle. The MCB code was equipped with JEFF3.2 nuclear data libraries for neutron transport simulations. The reactor core was divided into four radial and 10 axial fuel zones, which gives a total of 40 fuel zones. The geometrical parameters of the core and the TRISO fuel are presented in Tables 2 and 3, respectively.

Table 4 shows four versions of the homogenized thorium-uranium fuel composition. The main criterion is a similar mass of fissionable ^{235}U in the fresh reactor core – about 205 kg. This may be achieved by a variation of the input parameters for the volumetric homogenization method, i.e. kernel radius, weight fraction of each dioxide in the dioxide mix, enrichment and packing fraction.

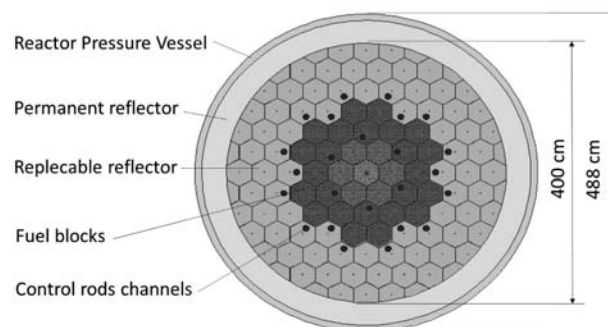


Fig. 1. Radial cross-cut of the reactor core.

Table 2. Main geometrical parameters of the core

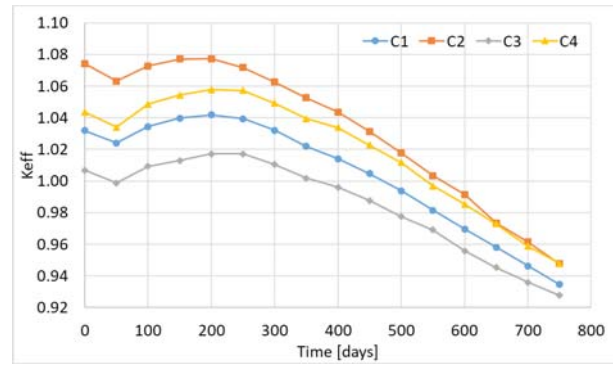
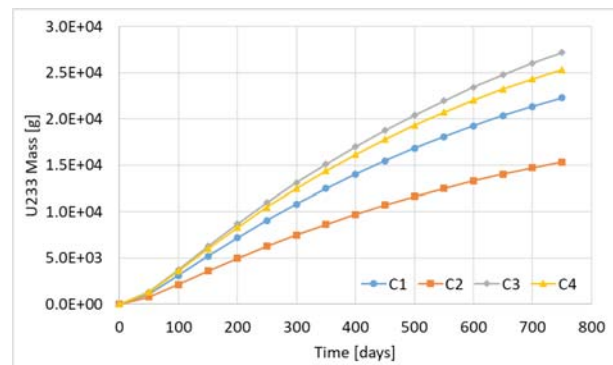
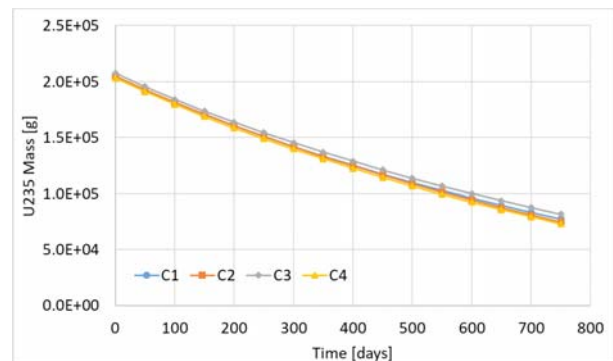
Reactor core	
Baffle radius (cm)	200
Active height (cm)	800
Reflector thickness (top/bottom) (cm)	120/160
Number of blocks (without CR/with CR)	250/60
Number of CR (core/reflector)	12/18
Fuel block	
Apothem (cm)	18
Height (cm)	80
Number of cooling channels per block:	
– without CR: small/large	6/102
– with CR: small/large	7/88
Cooling channel radius (small/large) (cm)	0.635/0.8
Pitch (cm)	1.88
Radius of CR channel (cm)	6.5
Radius of fuel channel (cm)	0.635
Number of fuel channels (without CR/with CR)	216/182
Fuel compact	
Radius (cm)	0.6225
Height (cm)	5

Table 3. Geometry of TRISO particles

TRISO	Thickness (mm)	Density (g/cm ³)
Fuel	600/700 (diameter)	10.42 (UO ₂)/9.5 (ThO ₂)
BPC	95	1.05
IPyC	40	1.90
SiC	35	3.18
OPyC	40	1.90

Figure 2 shows the evolution of K_{eff} for the investigated cases. The shapes of the curves are similar in each case. At the beginning, the decrease in K_{eff} due to the formation of absorbing fission products is observed. Then, K_{eff} increases to its peak value at about 200 days of irradiation due to the breeding of ²³³U, ²³⁹Pu and ²⁴¹Pu from residual ²³²Th and ²³⁸U. Afterwards, K_{eff} starts to decrease because of the ongoing fuel burnup. The highest values of K_{eff} were observed in the case C2 with the lowest mass of Th in the reactor core because of the lower fuel kernel radius. Although the mass of thorium for the subsequent cases C4 and C1 is similar, the relative values of K_{eff} are different; this difference originates from the variations in the initial ²³⁸U mass, which is lower in the case C4. The lowest values for K_{eff} were obtained in the case C3, characterized by the highest volume of ²³²Th and ²³⁸U.

The evolution of ²³³U bred from ²³²Th is presented in Fig. 3. The mass of the produced ²³³U depends strictly on the initial mass of ²³²Th. The higher the

**Fig. 2.** Evolution of K_{eff} .**Fig. 3.** Evolution of ²³³U.**Fig. 4.** Evolution of ²³⁵U.

initial mass of ²³²Th, the faster the production of ²³³U because of the higher absorption macroscopic cross section of ²³²Th. Therefore, the fastest production of ²³³U occurs in the case C3 and the lowest is observed in the case C2. The decrease of ²³⁵U due to the fuel burnup is shown in Fig. 4. The characteristics of all cases C1–C4 are similar due to the presence of almost the same amount of fissionable ²³⁵U in the reactor core. The initial mass of ²³⁵U decreases by about 60% during the irradiation period of two years. The production of ²³⁹Pu depends on the initial mass of ²³⁸U, as shown in Fig. 5. The case C4 with the lowest

Table 4. Fuel parameters for the volumetric homogenization method

Case	r_{KR} (cm)	$w^{\text{UO}_2, \text{FR}}$ (wt%)	$w^{\text{ThO}_2, \text{FR}}$ (wt%)	$w_i^{\text{U}^{235}}$ (%)	P (%)	Mass ²³⁵ U (kg)	Mass ²³⁸ U (kg)	Mass ²³² Th (kg)
1	0.35	50	50	20	15	204.76	816.46	1018.70
2	0.30	40	60	20	15	205.05	820.22	681.43
3	0.35	55	45	20	17	207.68	832.01	1267.00
4	0.35	60	40	25	15	203.35	610.04	1216.20

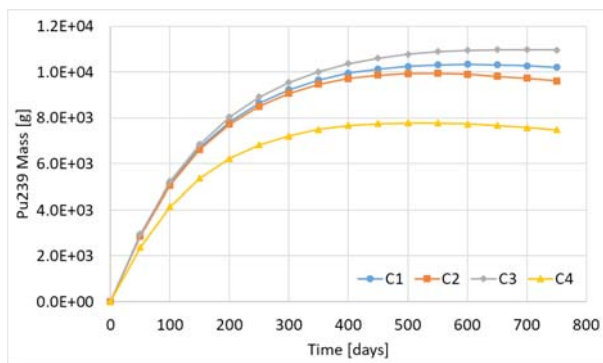


Fig. 5. Evolution of ²³⁹Pu.

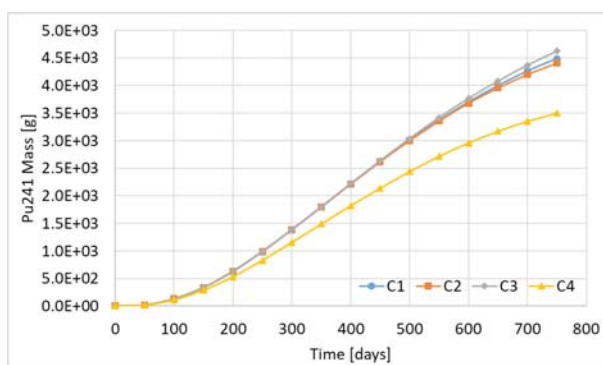


Fig. 6. Evolution of ²⁴¹Pu.

initial mass of ²³⁸U shows the lowest production of ²³⁹Pu and ²⁴¹Pu (Fig. 6). The production of ²³⁹Pu and ²⁴¹Pu is similar in other cases, where the initial mass of ²³⁸U is similar. However, during the ongoing fuel burnup, a difference in the shapes of the plutonium curves appears, which is related to the depletion of fissionable ²³⁵U and its replacement by ²³³U and plutonium isotopes as secondary fuel. This process is unambiguously observed in the case C2, where the mass of ²³⁹Pu starts to decrease after reaching its peak at about 500 days of irradiation. In this case, the production of ²³³U is the lowest; therefore, ²³⁵U is replaced by fissionable plutonium isotopes, mainly ²³⁹Pu.

Conclusions


The volumetric homogenization method for the modelling of the MHTR core was presented in this study. This method was applied for the numerical Monte Carlo modelling of neutron transport in the MHTR core with thorium-uranium fuel. The example results of the modelling were presented. The results prove the reliability of the method for the initial screening of the reactor core performance. The universal character of this method makes it suitable for the numerical modelling of any type of material fuel composition and geometry. Thus, the method can be used not only for the MHTR modelling but also for the modelling of any fissionable system with a complicated fuel geometry, especially using linear chain method [8]. Further study on this method will focus on benchmarking with a full 3D MHTR core model with double heterogeneity of the TRISO fuel. This will allow the verification

of the simplified models developed and their use as a replacement of detailed models. In the benchmarking process, the condition under which a defined replacement may happen will be also determined. The benchmarking will define the areas of the reactor core physics that can be reliably modelled using the volumetric homogenization method, e.g. radiotoxicity of the spent nuclear fuel [9], which may facilitate the whole MHTR design methodology.

Acknowledgments. The research was partially supported by PL Grid Infrastructure, available at the Academic Computer Centre CYFRONET AGH. Additionally, partial financial support under the scientific subvention 16.16.210.476 by the Polish Ministry of Science and Higher Education is kindly acknowledged.

ORCID

J. Cetnar  <http://orcid.org/0000-0002-0163-3331>

M. Oettingen  <http://orcid.org/0000-0001-7499-7585>

References

1. Talamo, A., Ji, W., Cetnar, J., & Gudowski, W. (2006). Comparison of MCB and MONTEBURNS Monte Carlo burnup codes on a one-pass deep burn. *Ann. Nucl. Energy*, 33(14/15), 1176–1188. doi.org/10.1016/j.anucene.2006.08.006.
2. International Atomic Energy Agency. (2012). *Role of thorium to supplement fuel cycles of future nuclear energy systems*. Vienna: IAEA. (Nuclear Energy Series NFT-2.4).
3. International Atomic Energy Agency. (2005). *Thorium fuel cycle – Potential benefits and challenges*. Vienna: IAEA. (IAEA-TECDOC-1450).
4. Shamanin, I. V., Grachev, V. M., Chertkov, Yu. B., Bedenko, S. V., Mendoza, O., & Knyshev, V. V. (2018). Neutronic properties of high-temperature gas-cooled reactors with thorium fuel. *Ann. Nucl. Energy*, 113, 286–293. DOI: 10.1016/j.anucene.2017.11.045.
5. Oettingen, M., & Stanisiz, P. (2018). Monte Carlo modelling of Th-Pb fuel assembly with californium neutron source. *Nukleonika*, 63(3), 87–91. DOI: 10.2478/nuka-2018-0011.
6. Cetnar, J. (2006). Solution of Bateman equations for nuclear transmutations. *Ann. Nucl. Energy*, 33, 640–645. DOI: 10.1016/j.anucene.2006.02.004.
7. Oettingen, M., Cetnar, J., & Mirowski, T. (2015). The MCB code for numerical modelling of fourth generation nuclear reactors. *Computer Science*, 16, 329–350. DOI: 10.7494/csci.2015.16.4.329.
8. Cetnar, J., Stanisiz, P., & Oettingen, M. (2021). Linear chain method for numerical modelling of burnup systems. *Energies*, 14, 1520. https://doi.org/10.3390/en14061520.
9. Oettingen, M. (2021). Assessment of the radiotoxicity of spent nuclear fuel from a fleet of PWR reactors (2021). *Energies*, 14, 3094. https://doi.org/10.3390/en14113094.

Appendix I – List of symbols**Volumes (cm³)**

V^{KR}	Volume of TRISO kernel (fuel volume)
V_i^{TRISO}	Volumes of TRISO materials around kernel
V^{COM}	Volume of fuel compact
V^{TRISO}	Volume of TRISO particle
$V^{TRISOinCOM}$	Volume of TRISO particles in the compact
$V_i^{TRISO,FR}$	Volume fraction of TRISO materials in the compact

Lengths (cm)

r_{KR}	Kernel radius (fuel radius)
r_i	Kernel radius r_{KR} increased by material layer thickness t_i
t_i	Material layer thickness
r_{COM}	Radius of fuel compact
h_{COM}	Height of fuel compact
r_{TRISO}	Radius of TRISO particle

Densities (g/cm³)

ρ^{HOMO}	Density of homogenized compact material
ρ_i^{COM}	Densities of compact materials
$\rho^{(HM)O_2}$	Density of mixed dioxides
$\rho_i^{(HM)O_2}$	Density of each dioxide

Masses (g)

m_i^{COM}	Mass of each material in the compact
m^{COM}	Mass of the compact

Weight fractions (–)

$w_i^{COM,FR}$	Weight fraction of each material in the compact
$w_i^{(HM)O_2,FR}$	Weight fractions of each dioxide in the dioxide mix
w_i^U	Weight fractions of uranium isotopes in uranium
w_i^{ISO}	Weight fractions of isotopes in no-fuel compact materials

$w_i^{HOMO,ISO}$ Weight fractions of isotopes in homogenized material mix for non-fuel materials

$w_i^{HOMO(HM)O_2}$ Weight fractions of isotopes in homogenized material mix for fuel

$w_i^{(HM)O_2}$ Weight fractions of each isotope in heavy metal dioxide

Atom fractions (–)

a_i^U Atom fractions of uranium isotopes in uranium

$a_i^{(HM)O_2}$ Atom fractions of each isotope in heavy metal dioxide

$a_i^{(HM)O_2,FR}$ Atom fractions of each dioxide in the dioxide mix

a_i^{ISO} Atom fractions of isotopes in no-fuel compact materials

Atomic weights (g/mol)

M_i^U Atomic weights of each uranium isotope

\bar{M}^U Average atomic weight of uranium for given enrichment

$\bar{M}^{(HM),MIX}$ Average atomic weight of the dioxide mix

$M_i^{(HM)O_2}$ Atomic weights of each dioxide

M^{HM} Atomic weight of heavy metal

M^O Atomic weight of oxygen

M_i Atomic weights of other no-fuel isotopes of compact materials

\bar{M} Average atomic weight of other no-fuel elements in compact materials

$\bar{M}^{(HM)O_2}$ Average atomic weights of each dioxide

Others

N^{TRISO} Number of TRISO particles in the fuel compact (–)

$N_i^{(HM)O_2}$ Average numbers of atoms of each isotope in uranium dioxide (–)

$N^{(HM)O_2}$ Number of atoms in the dioxide molecule (–)

P Packing fraction (%)

TRISO TRI-structural ISotropic.